Truncation Error Estimates for Refinement Criteria in Nested and Adaptive Models

WILLIAM C. SKAMAROCK

National Center for Atmospheric Research, Boulder, Colorado*

(Manuscript received 3 May 1988, in final form 7 November 1988)

ABSTRACT

Truncation error estimates are considered as criteria for fine-grid placement and movement in nested and adaptive finite-difference atmospheric models. A simple method for calculating the truncation error at any time during an integration is described. Two cases using the shallow-water equations and the hydrostatic primitive equations are examined to demonstrate the accuracy of the method and illuminate the relationships among the truncation error, a particular discretization, the equations being solved and the flow physics. The relationship between the truncation error and the solution error is also discussed and it is argued that minimization of the truncation error is the necessary consideration for producing more accurate numerical solutions. Examples of use of the truncation error estimates in adaptive models are also presented.

1. Introduction

Numerical models of the atmosphere are becoming increasingly sophisticated. Nested models in which the fine grids may move and adaptive models in which the number, size and location of fine grids may change bring about the problem of choosing suitable criteria to use for deciding where to place the fine grids. In this paper a method for calculating the truncation error in finite difference simulations of atmospheric flow is presented and possibilities for using the truncation error estimates for fine grid placement are discussed. These estimates have been used in the adaptive hydrostatic primitive equations model of Skamarock et al. (1989) and Skamarock (1988a) and in the adaptive nonhydrostatic model of Skamarock (1988b). The results and conclusions presented here are, in part, based upon the results from the adaptive models.

First, criteria presently used for fine-grid placement in atmospheric models will be considered. Adaptive grid refinement techniques have been under development for a variety of engineering and aerodynamic flow calculations and techniques used in these contexts will also be discussed. Few of these techniques make use of estimates of the truncation error or overall solution error as refinement criteria. Rather they rely on measures of the solution gradient, second derivatives or some combination of the two.

A method for calculating estimates of the truncation errors which arise from the discretization of hyperbolic systems of equations is outlined in section 3. The method has been used previously by Berger and Oliger (1984) in the course of developing the grid-refinement technique later used by Skamarock et al. (1989) for computing large-scale atmospheric flow. It is a simple method in which one need not know the form of the truncation error and its implementation does not require excessive amounts of additional programming. Accurate estimates of the truncation error associated with the discretization of the evolving flow field may be obtained and used as criteria for fine-grid placement. The accuracy of the estimate has been demonstrated by Skamarock et al. and data from those calculations will be used to further demonstrate the accuaracy of the procedure. The relationship among the equations being solved, a particular discretization, and the truncation error in two large-scale flow simulations will be examined.

Truncation error estimates can also be used for purposes other than the placement of fine grids. Solution methods for PDEs have an inherent accuracy commonly referred to as their order of accuracy, the overall accuracy of the method being the lowest order of accuracy in the differencing of the individual terms in the equations being discretized. In reasonably constructed schemes, most terms are differenced with methods having accuracy of the same order. Discretization decisions are often based on a modeler's intuition or the ease of implementation and not necessarily on the actual effect of the discretization on the solution in terms of solution error—the ultimate arbitrator. While the errors associated with individual terms are considered to be of the same relative size, the contribution to the total truncation error in a numerical scheme varies widely among the truncation errors associated with the discretization of particular terms. Truncation error formulas can be derived that reveal more information about the source of the truncation errors. This new information can be used to derive

* The National Center for Atmospheric Research is sponsored by the National Science Foundation.

Corresponding author address: William C. Skamarock, NCAR, P.O. Box 3000, Boulder, CO 80307-3000.

more straightforward techniques for computing estimates of the truncation error, i.e., computing the finite difference representation of the terms, and it can also be used to indicate which terms may need more accurate discretization.

Last, the use of actual truncation error estimates in atmospheric flow computations using adaptive or nested models is discussed. The development of the next generation of models which use adaptive and more sophisticated nesting techniques is underway, particularly in the research community. Some techniques for making use of the truncation-error estimates are presented. Even when adaptive or nested modeling techniques are not being used, the truncation-error estimates can provide information concerning solution accuracy, information which until now has not been available. Using truncation-error estimates to determine the quality of solutions directly may be the most important use of the error estimating technique in atmospheric calculations at present.

2. Review of refinement criteria

There are few atmospheric models which can make use of information concerning solution quality for solution refinement. In general, ad hoc methods are used for fine-grid placement in nested models. Fine grids are placed over regions where finer resolution is desired rather than over regions where refinement is necessary for an overall more accurate solution. Nothing can be said about the accuracy of these nested model solutions other than that the truncation error of the scheme is lower in the refined region. It can not be stated with any certainty that the overall solution is more accurate or even that the solution in the refined region is more accurate because no measure of the solution error or truncation error is used or even calculated.

Some moveable fine-grid tropical-cyclone models use objective criteria to determine the location of the fine grids (see Harrison 1973; Jones 1977; Kurihara and Bender 1980). The fine grids are centered over the cyclone. The cyclone center is defined as being either the surface-pressure low or the first moment of the difference of the surface pressure from some mean pressure. Consistent results have been obtained from these models because it is most often the case that very little is happening outside the region occupied by the cyclone. The errors in the numerical scheme are largest within the cyclone and refinement should occur there. This is an example of using knowledge of the flow to place fine grids. If the relative evolution of the flow is known beforehand, as is often the case with tropical cyclone simulations and in models used in research applications, using previous experience and knowledge is often the preferred and certainly the most expedient technique for placing fine grids. For operational use, experience and reliance on the identification of flow features may not be adequate because it may not be known beforehand how the solution will evolve. There is no obvious way to extend the use of this criteria to more general flows.

In the engineering disciplines, adaptive techniques are being actively developed using both finite-difference and finite-element methods. The finite-element applications deal with elliptic and parabolic PDEs and refinements consist of a reconstruction and/or addition of elements. Elements needing refinement are identified by computing some measure of the solution error. These error estimates are often similar to truncation errors in appearance. The error-estimation techniques for the adaptive finite-element methods are mostly problem specific and error-estimate derivations are not straightforward or without many assumptions and qualifications. There are few finite-element models for atmospheric-flow computations and none of these are adaptive. No more will be said about these methods but interested readers can refer to Babuška et al. (1983) for more details about adaptive finite element models.

Adaptive methods using finite-difference techniques, as opposed to adaptive finite-element methods, in general do not use concrete measures of the solution error. Most of the finite-difference techniques refine in regions where derivatives are large. Dwyer et al. (1980) describe an adaptive procedure which places grid points in proportion to solution gradients. The method is a global-refinement technique because new points are not added; rather, existing points are redistributed based upon the evolving solution. Physical space is mapped to computational space $(x, y, t \rightarrow \xi, \eta, T)$ using

$$\xi(x, y, t) = \frac{\int_0^S \left(1 + b\left|\frac{\partial T}{\partial S}\right| + C\left|\frac{\partial^2 T}{\partial S^2}\right|\right) dS}{\int_0^{S_{\max}} \left(1 + b\left|\frac{\partial T}{\partial S}\right| + C\left|\frac{\partial^2 T}{\partial S^2}\right|\right) dS}$$

where b and C are constants or functions that control the relative importance of the first and second derivatives. Here S is the arc along which the points (increments of ξ) are to be placed. For example, if $b = C = 0$, a uniform distribution of points along the arc S is obtained. Larger values of b and C lead to the placement of more points around the larger values of the first and second derivatives of the dependent variable T.

As noted earlier, methods that do not make use of actual error estimates have no formal way of controlling errors in the solutions. Solution accuracy can be guaranteed, in a strict sense, only by using accurate estimates of the error induced by the discretization. Methods which use derivatives, such as Dwyer et al. (1980), have proven successful in problems involving shocks and very strong fronts. They perform calculations for combustion problems involving flame fronts and also for 2-D (two-dimensional) convection and convection-diffusion problems. As with the cyclone calculations, flow features that lead to large errors are obvious and

this knowledge is easily used. In more complex flows the connection of flow features to errors may not be obvious.

A more sophisticated refinement technique has been developed by Dannenhoffer and Baron (1986). They solve the steady state 2-D Euler equations adaptively for flow around an airfoil using a local-refinement procedure; gridpoints (in this case cells) are added to the mesh as opposed to redistributing the existing points. The principal features present in the flows are strong shocks; hence, solution gradients are used for refinement criteria. As with the technique developed by Dwyer et al. (1980), there is no direct measure of the solution error and the accuracy of the solution cannot be guaranteed in a strict sense. The solution is considered sufficiently accurate based upon the convergence parameters on two successive grids.

The Dannenhoffer and Baron technique is of interest because it makes use of an expert system to control the adaptation. The expert system incorporates rules that are used to decide which cells should be divided based on the refinement criteria. The system also contains rules that allow for error recovery. If a refined grid will not yield a converged solution, i.e., the solution process diverges, then the grid will be altered (rerefined) using knowledge contained in the rules incorporated in the expert system. Nonconvergence is usually the result of failure to refine certain portions of the grid. Additional rules are used to determine where further refinement may be necessary to bring about convergence even though the original refinement criteria may not indicate such refinement is necessary. Dannenhoffer and Baron consider the optimal refinement criteria for calculations of transonic flow to be the gradient of the density.

Knowledge of the flow can and should be used as refinement criteria, but it should not be used in place of knowledge of the actual error in the solution. Combining both kinds of information will be important in future adaptive models. In section 3 a technique is described for obtaining estimates of the truncation error in finite difference schemes that is not problem dependent or discretization dependent. The technique, developed by Berger and Oliger (1984) differs from the methods discussed in this section (for finite difference models) in that the errors being measured are directly tied to the solution error.

3. Truncation error estimates based upon Richardson extrapolation

In developing adaptive schemes or any approximate solution technique, we wish to minimize the solution error. Unfortunately, the solution error is very difficult if not impossible to determine during an integration. Truncation errors associated with methods are easier to compute. Examination of the relationship between solution error and truncation error show that truncation error is the source of solution error; minimization of the solution error can only be attained by continually minimizing the truncation errors. In this section a method for estimating the truncation error is presented but first we examine the relationship between the truncation error and the solution error.

Given a set of hyperbolic PDEs

$$u_t = L[u]$$

where L is a spatial differential operator and u may be a vector, a space and time discretization of this set can be written as

$$\mathbf{u}(x, t + k) = Q_{h,k}[u(x, t)], \tag{3.1}$$

where $\mathbf{u}$ is the approximate solution at time $t + k$, $Q_{h,k}$ is an operator representing the discretization, and h and k are the space and time step sizes respectively. The truncation error for the discretization is derived by substituting the continuous solution, represented as a Taylor series valid locally about a point (x, t), into the finite difference equations (3.1). If we assume that u is sufficiently smooth, i.e. no discontinuities and reasonably small h and k, then the truncation error τ can be written

$$\begin{aligned}\tau &= u(x, t + k) - Q_{h,k}[u(x, t)] \\ &= k[k^{q_1}a(x, t) + h^{q_2}b(x, t)] + kO(k^{q_1+1} + h^{q_2+1}) \\ &= \tau_L + kO(k^{q_1+1} + h^{q_2+1}).\end{aligned} \tag{3.2}$$

Here τ_L is the leading order term in the truncation error τ, q_1 and q_2 are the orders of accuracy in space and time, respectively, and $a(x, t)$ and $b(x, t)$ are usually higher-order derivatives of u.

The truncation error τ is not equivalent to the solution error. The truncation error is the error in approximating the differential equation at a point whereas the solution error is the error in the solution itself. The solution error at time $t + k$ can be defined as

$$e(x, t + k) = u(x, t + k) - \mathbf{u}(x, t + k). \tag{3.3}$$

After the initial time step the solution error at a point is equal to the truncation error at that point [compare (3.2) and (3.3) using (3.1)], or stated differently, the solution error introduced in the first time step is exactly equal to the truncation error of the scheme at that time step.

After a second time step the solution error is

$$e(x, t + 2k) = u(x, t + 2k) - \mathbf{u}(x, t + 2k). \tag{3.4}$$

The relationship between the solution error and the truncation error can be recovered by noting that the approximate solution, $\mathbf{u}(x, t + 2k)$ can be represented as

$$\begin{aligned}\mathbf{u}(x, t + 2k) &= Q_{h,k}[\mathbf{u}(x, t + k)] \\ &= Q_{h,k}[u(x, t) - e(x, t + k)] \\ &= Q_{h,k}[u(x, t) - \tau(x, t + k)].\end{aligned}$$

Here $\tau(x, t+k)$ is the truncation error associated with the time step $t \rightarrow t+k$. Substituting this into (3.4) yields the solution error after the second time step.

$$e(x, t+2k) = u(x, t+2k) - Q_{h,k}[u(x, t) - \tau(x, t+k)]. \quad (3.5)$$

If the equations are linear, then the expression for the solution error can be further simplified:

$$e(x, t+2k) = u(x, t+2k) - Q_{h,k}[u(x, t+k)] + Q_{h,k}[\tau(x, t+k)].$$

Recognizing that the first two terms on the RHS of this equation comply with our definition of a truncation error (Eq. 3.2), the solution error for a linear system becomes

$$e(x, t+2k) = \tau(x, t+2k) + Q_{h,k}[\tau(x, t+k)]. \quad (3.6)$$

For example, if we were solving a linear advection-diffusion equation, the solution error would be the truncation error introduced in the previous step plus the advected and diffused truncation errors that were introduced into the solution before the last time step.

The interaction between the truncation error and the solution error for a nonlinear system, given by Eq. (3.5), cannot be interpreted in such a simple manner as in the case of the linear system because in the nonlinear system the truncation error interacts with the evolving solution. Specifically, the truncation error $\tau(x, t+2k)$ is a function of $\tau(x, t+k)$. However, an appropriately linearized nonlinear system will describe how the nonlinear system will behave over the time period for which the linearization is valid. If the solution is reasonably smooth and h and k are reasonably small then the truncation and solution errors of the linearized system will approximate the truncation and solution errors of the nonlinear system for at least a few time steps.

Equations (3.5) and (3.6) show that the source of the solution error associated with the discretization is the truncation error. Grid refinement in regions of high solution error cannot guarantee a reduction in the solution error whereas grid refinement in regions of high truncation error decrease the truncation error and decrease the solution error. Truncation error should dictate where refinement occurs. A more rigorous argument is presented by Oliger (1984) in the context of adaptive mesh refinement.

The solution error is difficult to compute, but as we have noted it is the truncation error that should guide refinement. A simple method for computing the truncation error based on Richardson extrapolation was first used by Berger and Oliger (1984) in an adaptive solution method for hyperbolic PDEs. The adaptive method and truncation-error estimate technique was later used by Skamarock et al. (1989) in the solution of the 3-D hydrostatic primitive equations.

We use the assumption of a smooth solution, i.e., the existence of a valid local linearization to derive the truncation error estimate. By taking two time steps on a grid of step sizes h and k, and assuming that the time and space differencing are of the same order of accuracy ($q_1 = q_2$), the solution error for the linear system given by Eq. (3.6) can be rewritten

$$u(x, t+2k) - Q^2_{h,k}[u(x, t)] = 2\tau_L + kO(k^{q+1} + h^{q+1}). \quad (3.7)$$

Here we have used the assumption of a reasonably smooth solution to replace $\tau(x, t+2k)$ and $Q_{h,k}[\tau(x, t+k)]$ with $\tau_L + kO(k^{q+1} + h^{q+1})$.

Next, a single time step of $2k$ is taken on a grid with step size $2h$.

$$u(x, t+2k) - Q_{2h,2k}[u(x, t)] = 2^{q+1}\tau_L + kO(k^{q+1} + h^{q+1}). \quad (3.8)$$

Subtracting (3.7) from (3.8) and normalizing by the appropriate constant yields the estimate of the leading order term in the truncation error.

$$\tau_L = \frac{Q^2_{h,k}[u(x, t)] - Q_{2h,2k}[u(x, t)]}{2^{q+1} - 2} + kO(h^{q+1} + k^{q+1}). \quad (3.9)$$

This is the truncation error estimate formula valid for both linear and nonlinear systems. The technique requires taking two time steps on the base grid and a single time step on a grid with grid lengths of $2h$ and $2k$. Subtraction and appropriate normalization yield the truncation error estimate.

There are advantages in using this technique as opposed to calculating the truncation error by other means. The exact form of the truncation error need not be known because $a(x, t)$ and $b(x, t)$ are never calculated. Also, the same solver that is used to advance the equations can be used to compute the estimate of the truncation error. Thus, the truncation error is easy to compute even for systems containing several variables.

One drawback of the method is that the spatial and temporal discretizations must be of the same order. This is true for many schemes but when it is not true a more expensive variant of the above method can be used. The variant involves keeping the time step fixed and using Eq. (3.9), with $Q_{2h,k}$ replacing $Q_{2h,2k}$ and $Q_{h,k}$ replacing $Q^2_{h,k}$, to estimate the truncation error associated with the spatial discretization. Next, the space step is held constant and (3.9) is used with $Q_{h,2k}$ replacing $Q_{2h,2k}$. This gives the truncation error associated with the time discretization. These separate estimates of the space and time truncation errors can be added to determine the total truncation error or used

individually. The computational cost of using this variant is higher than the cost of the first method.

The general method produces an estimate of the truncation error accurate to $kO(h^{q+1} + k^{q+1})$ if the solution is reasonably smooth. In regions containing shocks, fronts, or other nonsmooth features the truncation-error estimates will be inaccurate but the estimates will likely be large and appropriately identify the regions as needing refinement. High accuracy is not necessary because the estimates are not used to correct the solution.

In practice, atmospheric models often use multiple time-level schemes. The finite-difference Eq. (3.1) on which the analysis is based encompasses only single time-level schemes. Multiple time-level schemes, such as the popular leapfrog method, require a different form for (3.1) if the analysis is to be carried through. The results are similar to those presented for the single time-level schemes and (3.9) can be used to estimate the truncation errors. In practice, if we apply (3.9) with a finite-difference scheme employing a leapfrog time discretization, the solution at times t, $t - k$ and $t - 2k$ would be required to perform the truncation error estimate using (3.9). The solution at $t - 2k$ and t are needed for the $Q_{2h,2k}$ operator and the solution at $t - k$ and t are needed for the $Q^2_{h,k}$ operator. The accuracy of the error estimates is retained and the variants of (3.9) used for separately computing the spatial truncation error estimates and the time truncation error estimates can also be used.

Finally, a comment on observations of truncation errors in nested and adaptive models is needed. Truncation errors and solution errors have been shown to decrease in adaptive models (using truncation errors as a guide to refinement) for solutions to simple hyperbolic systems (Berger and Oliger 1984) and the Navier-Stokes equations [laminar flow (Caruso 1985)]. In other adaptive simulations (Berger and Jameson 1985; Skamarock et al. 1989; Skamarock 1988b) the overall accuracy of the adaptive solutions have been determined by comparison to single fine-grid solutions, and in this way the adaptive methods have been justified. It is often the case, though, that the truncation errors are larger on the finest grids than on the coarser ones. In many models finer resolution often allows finer-scale structure to appear. This occurs most often when the filtering and smoothing in the model is proportional to the grid length. In these cases the necessary question to ask is, What is the correct solution? or, What is the grid-independent solution? and in the case where the filtering is dependent on the grid resolution an important question is, What equations are we actually solving?

Truncation errors should play a dominant role in determining where refinement occurs even in these cases, but the concept of minimizing the truncation error has to be reconsidered in the context of the previously posed questions.

4. Examination of truncation-error estimates

The following are examples of truncation-error estimates for particular flows and particular discretizations of the governing equations. The results are not applicable to all numerical schemes or all flows. The specific results may change for different discretizations or for flows which exhibit motion on different scales. The primary purpose of this section is to demonstrate that the Richardson truncation-error estimates are accurate, even for the pressure and temperature fields in hydrostatic primitive-equation models. These results are presented to illustrate how one can examine the Richardson error estimates and compute them in a simpler manner. Also considered is what might be learned from the estimates.

Two cases are used to examine the truncation error estimates. In the first case, the shallow-water equations are used to model a cyclone being advected by a zonal flow. While this case is similar to the case presented in Skamarock et al. (1989), the calculations differ because in this simulation a constant, uniform zonal wind is prescribed and no acceleration technique is used in the time-integration scheme. In the results of Skamarock et al. the dominant truncation errors are associated with the time-discretization scheme and the error is computed on a very coarse grid. These factors preclude the type of analysis that is performed for the present case.

a. *Shallow water equation example*

We can write the flux form of the shallow-water equations as

$$\frac{\partial h}{\partial t} = -\left[\frac{\partial (hu)}{\partial x} + \frac{\partial (hv)}{\partial y}\right] \tag{4.1}$$

$$\frac{\partial (uh)}{\partial t} = -\left[\frac{\partial (uuh)}{\partial x} + \frac{\partial (uvh)}{\partial y}\right] - \frac{g}{2}\frac{\partial h^2}{\partial x} + fvh \tag{4.2}$$

$$\frac{\partial (vh)}{\partial t} = -\left[\frac{\partial (uvh)}{\partial x} + \frac{\partial (vvh)}{\partial y}\right] - \frac{g}{2}\frac{\partial h^2}{\partial y} - fuh. \tag{4.3}$$

The horizontal velocities are u and v in the x and y direction, respectively, h is the free surface height, g the gravitational constant and f the Coriolis parameter. The equations are discretized on the C-grid illustrated in Fig. 1 and the simulation is on an f-plane ($f = 10^{-4}$ s^{-1}) in an east–west periodic channel. We can write the finite-difference form of the shallow-water set compactly using the following definitions:

$$(\alpha)_x = (\alpha_{i+1/2} - \alpha_{i-1/2})/\Delta x$$

$$(\alpha)_y = (\alpha_{j+1/2} - \alpha_{j-1/2})/\Delta y$$

$$\overline{(\alpha)}^x = (\alpha_{i+1/2} + \alpha_{i-1/2})/2$$

$$\overline{(\alpha)}^y = (\alpha_{j+1/2} + \alpha_{j-1/2})/2.$$

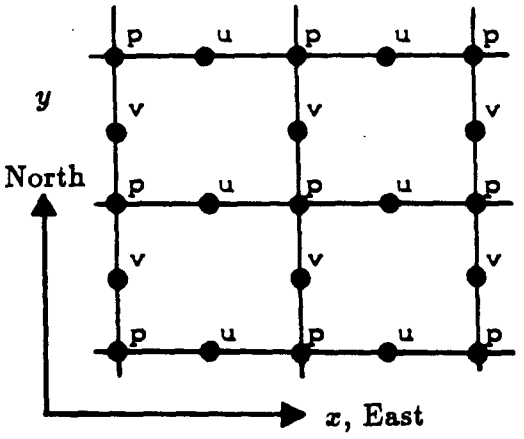

FIG. 1. C-Grid, h, π, T and ϕ are defined at the p points. Other terms u and v are the velocities in the x and y direction (east and north), respectively.

Using second-order centered differencing in time and space, the height tendency Eq. (4.1) is discretized as

$$\frac{h_{i,j}^{t+\Delta t} - h_{i,j}^{t-\Delta t}}{2\Delta t} = -[(\bar{h}^x u)_x + (\bar{h}^y v)_y], \quad (4.4)$$

the discretization for the u-momentum equation is

$$\frac{(uh)_{i,j}^{t+\Delta t} - (uh)_{i,j}^{t-\Delta t}}{2\Delta t} = -[(\bar{u}^x \overline{uh}^x)_x + (\overline{\bar{u}^y v \bar{h}^y}^x)_y] - (g/2)(h^2)_x + f\bar{h}^x \bar{v}^{yx}, \quad (4.5)$$

and the v-momentum equation is discretized in a similar manner.

The initial wind field is given by

$$U_T(x, y) = U_0 + U_c\left[\frac{(x - x_0)^2 + (y - y_0)^2}{L_c^2}\right]^{1/2} \times \exp\left[\frac{1}{2}\left(1 - \frac{(x - x_0)^2 + (y - y_0)^2}{L_c^2}\right)\right]. \quad (4.6)$$

and is depicted in Fig. 2. Here U_T is the tangential wind velocity for a cyclone centered at (x_0, y_0). The following results are for the case $U_c = 20$ m s^{-1}, $L_c = 500$ km and constant zonal wind $U_0 = 10$ m s^{-1}. The initial height field is found by taking the x and y derivative of (4.2) and (4.3), respectively, adding the results, setting $(uh)_x + (vh)_y = 0$, and solving the resulting Poisson equation for the free surface height h. Figure 3 shows the initial field for a 4000 km^2 channel with $\Delta x = \Delta y = 250$ km.

Figures 4 and 5 show the truncation errors in the u and h field, computed with the Richardson based technique using (3.4). The stable time step is dictated by the maximum gravity wave speed $u \pm \sqrt{gh}$ and not the maximum wind speed. A small time step is needed to satisfy the Courant condition; thus, the truncation errors resulting from the time discretization are small and the spatial discretization is responsible for most of

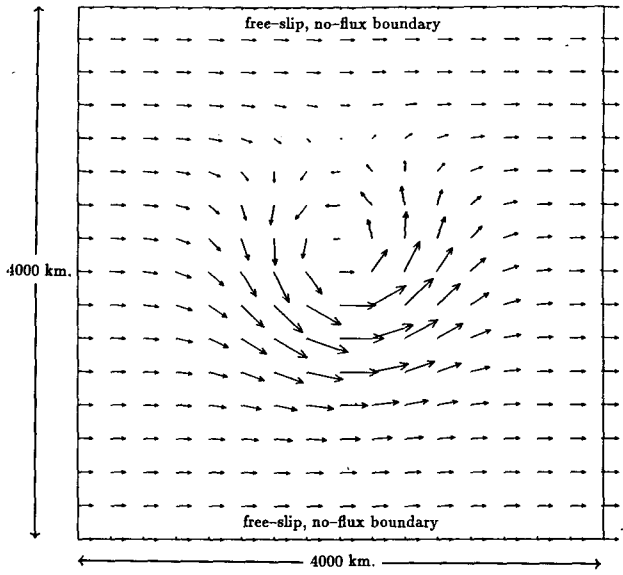

FIG. 2. Initial velocity field for shallow-water example. The region plotted is 4000 × 4000 km.

the error. The errors resulting from the spatial discretization can be computed directly using a variant of the Richardson technique described in section 3 and the results are virtually identical to those in Figs. 4 and 5 (given appropriate normalization).

What is striking about the truncation error estimates is that the truncation errors in the u-momentum equation are much smoother than for the height equation (4.1). In some sense this is counterintuitive because

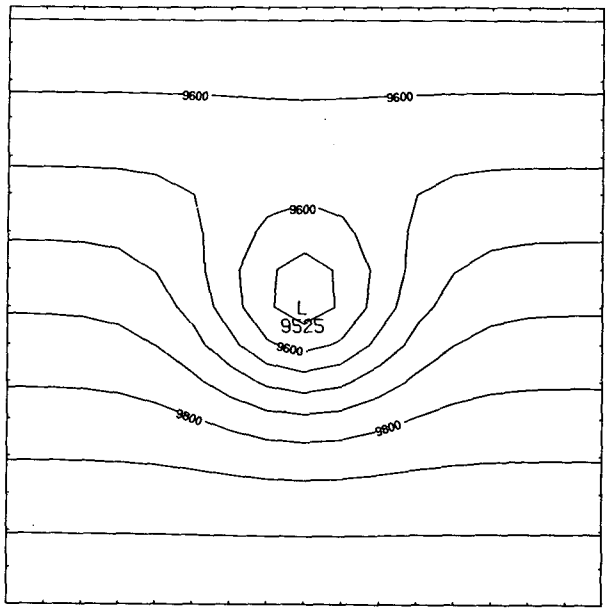

FIG. 3. Initial height field for shallow-water example. The height is in meters and the region plotted is the same as in Fig. 2.

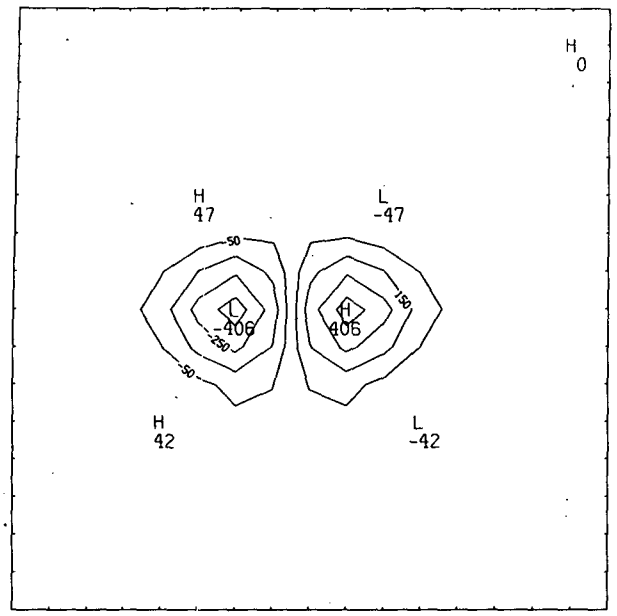

FIG. 4. Truncation-error estimate for the u-momentum equation using (3.9). Errors normalized and nondimensionalized by dividing by $\Delta t U_0 f$, $\times 10^4$.

one would expect the u-truncation error to exhibit a less smooth pattern given the greater number, and the nonlinearity of terms in the u-momentum equation as compared to the height tendency equation. We shall see that it is not the complexity of the overall discretization that results in nonsmooth error patterns, but rather, the discretization of the particular term that dominates the truncation error, and ultimately the dominant term in the exact truncation error formula, that determines the truncation error pattern.

The discretization for the right-hand-side of (4.1) given in (4.4), including the truncation error, can be written as

$$-\left[\frac{\partial(hu)}{\partial x}+\frac{\partial(hv)}{\partial y}\right]=-[(\bar{h}^{x}u)_x+(\bar{h}^{y}v)_y]$$
$$-\frac{\Delta x^2}{24}\Big[uh_{xxx}+vh_{yyy}+hu_{xxx}+hv_{yyy}$$
$$+\frac{3}{2}(u_x h_{xx}+h_x u_{xx}+v_y h_{yy}+h_y v_{yy})\Big]+O(\Delta x^3) \tag{4.7}$$

where the subscripts on the variables denote differentiation. Equation (4.1) and the truncation error contained in (4.7) can be nondimensionalized and scaled by defining nondimensional primed variables $u = Uu'$, $v = Uv'$, $h = H_0 + Hh'$, $x = Lx'$ and $y = Ly'$ with $H \ll H_0$. For large scale flows the RHS of (4.1) does not scale as UH_0/L, but rather scales as $R_0^2 UH_0/L$ for geostrophic flows and as $R_0 UH_0/L$ for synoptic scale flows; R_0 is the Rossby number and $R_0 \ll 1$. The leading-order terms in the truncation error can be found by substituting the dimensionless variables into the truncation error in (4.7). The leading order truncation error terms are

$$-\frac{\Delta x^2}{24}\frac{H_0 U}{L^3}(u'_{x'x'x'}+v'_{y'y'y'})+O\left(\frac{\Delta x^2}{24}\frac{HU}{L^3}\right). \tag{4.8}$$

These terms arise from the discretization of the divergence $(uh)_x + (vh)_y$.

Two observations may be made. First, if we compare the size of the mass divergence with the truncation error we find

mass divergence	truncation error
$R_0^2\frac{H_0U}{L}, R_0\frac{H_0U}{L}$	$\frac{\Delta x^2}{24L^2}\frac{H_0U}{L}$

For $R_0^2 \approx (\Delta x^2/24L^2)$, i.e., for very large scale flows simulated on a coarse grid, the mass divergence may be of the same relative size as the truncation error. It is unclear what the implications are for a numerical scheme which uses a nonzero quantity that is calculated with a scheme having an error that may be as large as the quantity itself. Even for synoptic-scale flows the errors can be significant compared to the mass divergence. In Skamarock (1988a) it was noted that the error estimates in the surface pressure fields and the temperature fields tended to be noisy, i.e., they contained many high-wavenumber components. This is not noise but rather the error in this case is less smooth than the flow which is being computed.

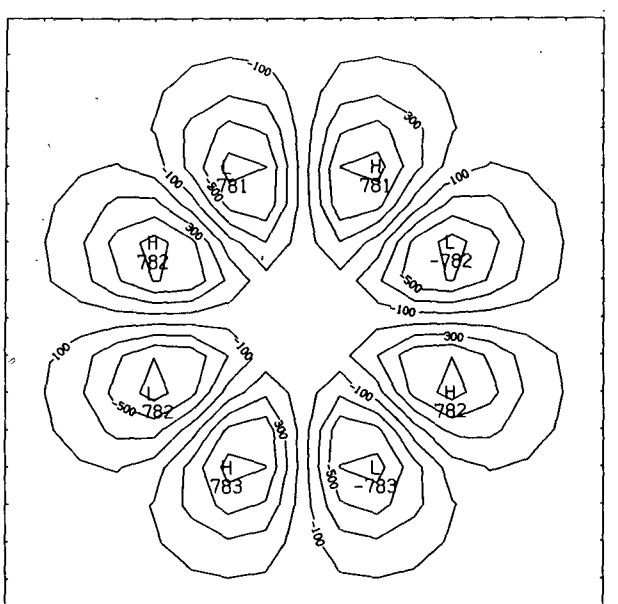

FIG. 5. Truncation error estimate for h using eqn. 3.9. Errors normalized and nondimensionalized by dividing by $\Delta t H_0 f$ where $H_0 = 10^4$ m, $\times 10^6$.

The Richardson estimate is accurate for sufficiently small h and k. This can be demonstrated by finite differencing the dimensional counterpart to (4.8) and computing the dominant contribution to the truncation error, or even more directly by using the analytic form of the initial wind field (4.6) and substituting it into (4.8). Either method produces results which verify the accuracy of the Richardson estimate.

The analytic form of the truncation error (4.7) indicates that the truncation error in the height field is due primarily to truncation errors in the calculation of the divergence of the velocity field. These truncation errors are proportional to $u_{xxx} + v_{yyy}$, and for simple flows can produce complex truncation error patterns. This information can be used in two ways: First, we now know that the truncation error in the discretization of the mass divergence can be reduced by a more accurate representation of the advecting velocities. Several more accurate schemes exist. A more accurate representation of the flux quantity h at the inflow and outflow faces will not improve the overall accuracy of the scheme. Second, the truncation error in the height calculations can easily be monitored throughout a computation by simply computing $u_{xxx} + v_{yyy}$. This is much simpler than the Richardson technique and may be used at any time with much less overhead than the Richardson technique.

The truncation error estimate for the velocity field u shown in Fig. 5 can be analyzed in a similar manner. Using a similar discretization for the hydrostatic primitive equations and for large-scale flow simulations, Skamarock et al. (1989) demonstrate that while the magnitude of individual terms in the momentum equations differ (the pressure gradient and Coriolis term tend to be an order or more of magnitude larger than the other terms, though they largely cancel each other), the truncation errors arising from the discretization of the terms tend to be the same relative size. This observation also holds for the shallow-water example. Table 1 lists the magnitude of the maximum truncation error associated with the individual terms for the shallow-water example. While the errors are of the same relative size, it turns out that the error in one term still dominates the overall truncation error. The dominant error is associated with the Coriolis term

$$\tau(fvh) = \frac{\Delta x^2}{8} f[vh_{xx} + h(v_{xx} + v_{yy})]$$

and the dominant error arises from the term $h(v_{xx} + v_{yy})$. For this flow and for the discretization of the u-momentum equation (4.5), we see that the truncation error in the u-momentum equation is much smoother than the truncation error in the height field equation The u-truncation error can also be computed in a very simple manner, i.e., by computing $(\Delta x^2/8) fh(v_{xx} + v_{yy})$.

TABLE 1. Maximum and average errors associated with the RHS terms in Eq. (4.2). Errors are nondimensionalized by multiplication with $(1/fU_0H_0)$.

Term	$\lvert\tau\rvert_{\max}$	$\int \lvert\tau\rvert\partial\Omega / \int \partial\Omega$
$\frac{\partial(uuh)}{\partial x}$	0.033	1.7×10^{-3}
$\frac{\partial(uvh)}{\partial x}$	0.041	1.7×10^{-3}
$\frac{g}{2}\frac{\partial(h^2)}{\partial x}$	0.010	6.6×10^{-4}
fvh	0.047	3.3×10^{-3}

b. *Hydrostatic primitive equations example*

In the primitive-equation calculations of Skamarock et al. (1988), a developing baroclinic wave was simulated. Truncation error estimates using (3.4) were used to place fine grids. An explicit time integration scheme was used, and the truncation errors arising from the temporal differencing are small; thus, we need consider only the errors arising from the spatial discretization. Errors in the vertical discretization are not computed or considered and no vertical refinement was used.

Truncation error estimates for the surface pressure, u velocity and temperature are examined next. The relevant equations are

$$\frac{\partial \pi}{\partial t} = -\sum_{k=1}^{K} \nabla\cdot(V\pi)\Delta\sigma_k \tag{4.9}$$

$$\frac{\partial(u\pi)}{\partial t} = -\left(\frac{\partial(\pi uu)}{\partial x} + \frac{\partial(\pi uv)}{\partial y} + \frac{\partial(\pi u\dot{\sigma})}{\partial \sigma}\right) - \frac{\partial(\pi\phi)}{\partial x} - (RT - \phi)\frac{\partial \pi}{\partial x} + \pi fv \tag{4.10}$$

$$\frac{\partial(T\pi)}{\partial t} = -\left(\frac{\partial(\pi uT)}{\partial x} + \frac{\partial(\pi vT)}{\partial y} + \frac{\partial(\pi T\dot{\sigma})}{\partial \sigma}\right) + \frac{RT}{\sigma}\omega + \pi Q \tag{4.11}$$

where

$$\omega = dp/dt = \pi\dot{\sigma} + \sigma(\partial\pi/\partial t + \mathbf{V}\cdot\nabla_\sigma\pi),$$

π is the surface pressure, and the equations are cast in the σ-coordinate system ($\sigma = p/\pi$) and are discretized on the C-grid.

The flow simulated in Skamarock et al. (1989) is a developing baroclinic disturbance which results from the perturbation of a baroclinically unstable jet. Three identical disturbances are initialized within an east–west periodic channel. There are no physics in the model and free-slip boundary conditions are used; thus, the flow is adiabatic. The domain size is 14 040 by 6480 km, $\Delta x = \Delta y = 360$ km and $\Delta t = 112.5$ s. Further information can be found in Skamarock et al.

The surface pressure π is given in Fig. 6 and a plot of the Richardson truncation-error estimate for π is presented in Fig. 7. Again, we see that the truncation error is not smooth and is dominated by high wavenumber components. The discretization of the surface pressure tendency equation is similar to that for the height tendency equation and can be written as

$$\frac{\pi_{i,j}^{t+\Delta t} - \pi_{i,j}^{t-\Delta t}}{2\Delta t} = -\sum_{k=1}^{K} [(\bar{\pi}^x u)_x + (\bar{\pi}^y v)_y]_k \Delta\sigma_k. \quad (4.12)$$

Here K is the number of layers in the model. The truncation error associated with this discretization will be similar to the error in the shallow-water calculations but here we must sum contributions to the error from all layers. The dominant term in the truncation error is

$$-\pi_0 \frac{\Delta x^2}{24} \sum_{k=1}^{K} (u_{xxx} + v_{yyy})_k \Delta\sigma_k, \quad (4.13)$$

where π_0 is an average surface pressure. The quantity (4.13) is plotted in Fig. 8. Again, the truncation error contains many high wavenumber components and can still be calculated easily using (4.13). The observations from the shallow-water model also apply to this more complex system.

In Skamarock et al., plots of the u-truncation error on the $\sigma = 0.3$ level (jet core) obtained using (3.4) and also computed directly from the exact truncation-error formula compare well and indicate that (3.4) does provide accurate truncation-error estimates. Figures 9 and 10 are the velocity vectors and the u-truncation-error estimate obtained using (3.4) for the $\sigma = 0.9$ level. Figure 10 also compares well with directly computed truncation-error estimates.

Complete truncation-error formulas and scalings for the momentum equation can be found in Skamarock et al. (1988) and are not repeated here. From the scaling analysis we expect that the truncation errors from the terms in (4.10) are of the same relative size. Table 2 presents the maximum size of the truncation errors associated with each of the terms in (4.10). Once again,

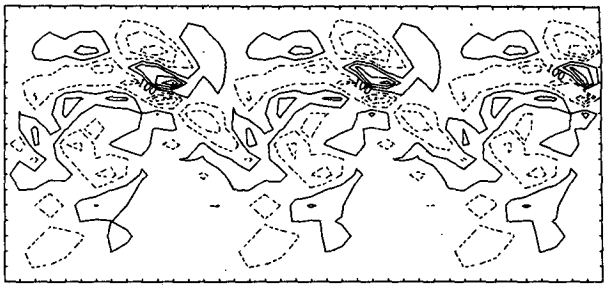

FIG. 7. Truncation error estimate for π Eq. (4.9) using (3.9). Errors normalized and nondimensionalized by dividing by $2\pi_0\Delta t/t^*$, where $t^* = 10^5$ s. Negative contours are dashed and the contour interval is 0.002 with minimum contours of ±0.001.

though, a single term can be found to dominate the truncation error—the Coriolis term. The discretization of the Coriolis term differs in this computation from the shallow-water computations. For the primitive equations solver, the discretization is

$$\pi f v = f\overline{\bar{v}^y \pi}^x$$

which results in a truncation error of

$$\tau(\pi f v) = \frac{\Delta x^2}{8} f(v\pi_{xx} + \pi(v_{xx} + v_{yy}) + 2\pi_x v_x).$$

Again, the dominant truncation error arises from the term $v_{xx} + v_{yy}$ even though the discretization is different. This is not surprising because the source of the truncation error arises from the interpolation of the v velocity and not the new specification of the flux quantity π. Figure 11 is a plot of the term $(\Delta x^2/8)f(v_{xx} + v_{yy})$. It is a good indicator of the form and magnitude of the truncation error. It should be noted that other terms contributing to the truncation error are significant.

The temperature on the $\sigma = 0.9$ surface is given in Fig. 12 and the error estimate in Fig. 13. Two observations can be made: First, the truncation error in the temperature (Fig. 13) is similar to the truncation error

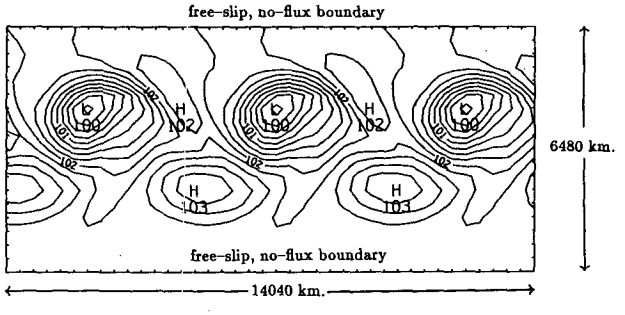

FIG. 6. Surface pressure (π) in millibars for primitive equations case. The domain plotted is 14 040 × 6480 km. and the contour interval is 2 mb.

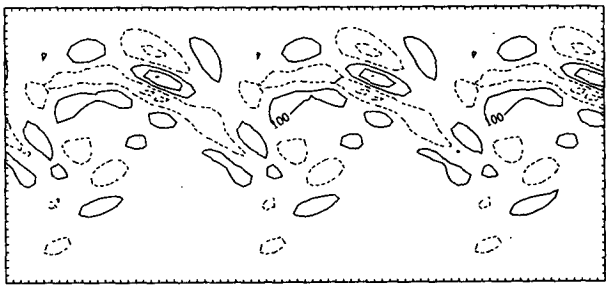

FIG. 8. Truncation error estimate for the pressure Eq. (4.9) computed using (4.13). Errors normalized and nondimensionalized by dividing by $2\pi_0/t^*$, and contouring is as in Fig. 7.

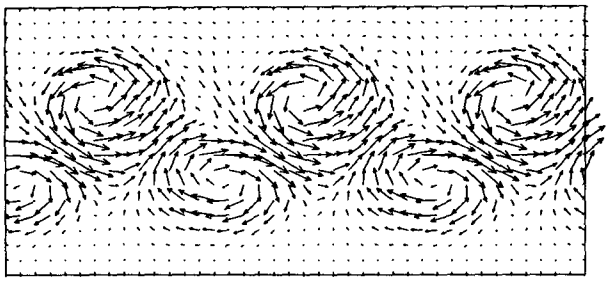

FIG. 9. Horizontal velocity on $\sigma = 0.9$ surface. The region plotted is the same as in Fig. 6.

TABLE 2. Maximum errors associated with the RHS terms in equation 4.10. Errors are nondimensionalized by multiplication with $(\tau/U_0\pi_0)$.

Term	$\lvert\tau\rvert_{max}$
$\frac{\partial(uu\pi)}{\partial x}$	0.119
$\frac{\partial(uv\pi)}{\partial x}$	0.146
$\frac{\partial(\pi\phi)}{\partial x} + (RT - \phi)\frac{\partial \pi}{\partial x}$	0.091
$f\pi v$	0.393

in the surface pressure (Fig. 7). This can be explained by noting that the temperature Eq. (4.11) is primarily an advection equation, as is the surface pressure Eq. (4.9). The errors will be similar because the temperature scales in the same manner as the surface pressure:

$$T = T_0 + \hat{T}T',$$

where $T_0 \gg \hat{T}$. The dominant source of error will be proportional to $\pi_0 T_0(u_{xxx} + v_{yyy})$. Note that here we do not sum over the layers. The T truncation error is similar to the π truncation error because the largest contribution to $u_{xxx} + v_{yyy}$ is at the lowest layer ($\sigma = 0.9$). We can also conclude that there are significant contributions to the truncation error from the other terms in the RHS of (4.11) because the largest term $(u_{xxx} + v_{yyy})$ is inaccurate in estimating certain portions of the overall truncation error. In particular, using $u_{xxx} + v_{yyy}$ as a truncation-error estimate results in missing part of the truncation error associated with the cold front.

Another conclusion is that whenever advected quantities have the form

$$A = A_0 + \hat{A}A' \tag{4.14}$$

with $A_0 \gg \hat{A}$, discretizations of the form (4.4) and (4.12) will result in truncation errors proportional to $u_{xxx} + v_{yyy}$. When advected quantities are not of the form (4.14) this will no longer hold and other terms in the truncation error will be important. The latter case will occur in the moisture advection equations and the truncation error will likely remain complex and could not be computed with a formula as simple as (4.13).

It is difficult to associate errors with particular flow features. This is not surprising given that the maximum truncation errors are associated with second and third derivatives of the horizontal velocities. It may be reasonable to associate large truncation errors with fronts, at least at the lower levels, though the figures show that not all frontal regions are associated with high error. It might seem reasonable to connect large errors with frontogenesis, but comparisons of the frontogenetical function calculated from the data (see Bluestein 1986) with the truncation errors do not necessarily provide a strong indication of where truncation errors are large. The connection of errors with frontal zones is linked to the wind shifts that make up the fronts. The largest truncation errors are associated with the warm front in these simulations and it is here that we find the greatest wind shifts. Truncation errors can only be associated with flow physics in so far as interesting flow phenomena are likely to contain regions in which there are large higher order derivatives; thus, interesting flow

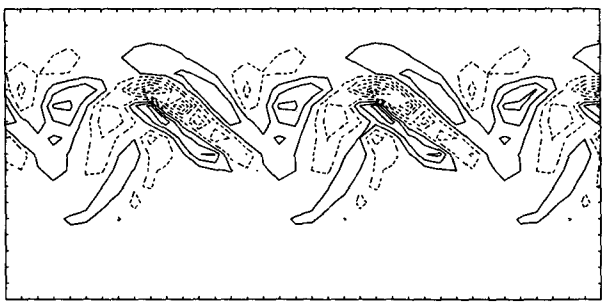

FIG. 10. Truncation error estimate for the u-momentum equation on the $\sigma = 0.9$ surface using Eq. (3.9). Errors normalized and nondimensionalized by dividing by $\Delta t U_0/t^*$ with $U_0 = 10\ \text{m s}^{-1} \times 10^3$. Negative contours are dashed and the contour interval is 0.1 with minimum contours of ± 0.05.

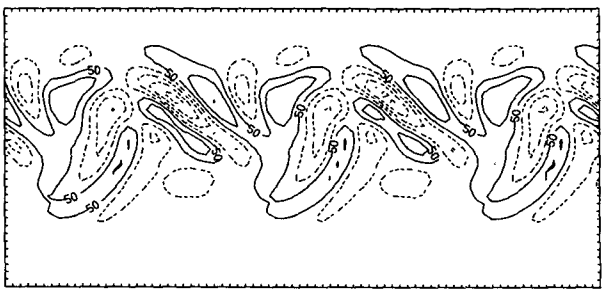

FIG. 11. Plot of $(\Delta x^2/8)f(v_{xx} + v_{yy})$ on the $\sigma = 0.9$ surface. Results are normalized and nondimensionalized by multiplication with t^*/U_0. Contours are as in Fig. 10.

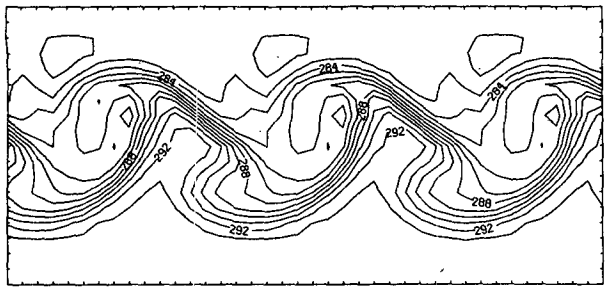

FIG. 12. Temperature field (K) on the $\sigma = 0.9$ surface. The region plotted is the same as in Fig. 6.

phenomena may possibly, but not necessarily, indicate locations of large truncation error.

Large truncation errors are not necessarily linked to regions of large gradients. This is very evident in the cases of the height Eq. (4.1) and surface pressure Eq. (4.9). Large values of the second derivatives could be used as a refinement guide for the momentum equations because of the discretization of the Coriolis term. This may not work in all cases, especially for smaller-scale flows where the Coriolis effect is smaller or for different (more accurate) discretizations of the Coriolis term. Techniques which rely on large first or second derivatives to identify regions of large truncation error will not always work and provide no direct connection to the solution error.

5. Using the truncation error estimates

The truncation error estimates obtained using the Richardson procedure can be used as refinement criteria during the solution process. First I reiterate the argument made in section 3 for using the truncation error as a guide for refinement. The error in the solution to a set of PDEs that arises from the discretization has the truncation error as its source. Localized truncation errors interact with the equations and become nonlocal solution error. The only way to control the overall accuracy of the numerical solution is to continually minimize the truncation error. Any other refinement criteria may miss regions of significant truncation error and lead to larger solution errors. Given that the first goal of numerical simulations is to produce accurate solutions to the continuous PDEs, minimization of the truncation error is paramount.

Of course, in numerical simulations of the atmosphere there are other sources of error. These include errors in initial data, boundary-condition specifications and boundary data, the parameterization of physical processes, and from other sources. It may be that these errors are more important than truncation errors in the solution of the PDEs. While this may be so, it can be difficult to judge the true effects of the other sources of error without accurate solutions to the PDEs; hence, accurate solution techniques are necessary. Increased resolution might also help decrease the errors from other sources. If this is the case then information concerning where increased resolution will help reduce these errors should be used in conjunction with the truncation error estimates.

Various criteria for choosing refinement regions in fluid dynamic calculations have been considered in section 2. More flexible solution processes can make use of the detailed error estimates and refine only in regions where error is large. In most nested models, flexibility is limited and the only choice one has is where to place—or where to move—an already existing fine grid(s). In some sense this is an easier problem for there are many fewer degrees of freedom; hence, the decision is easier to make (and easier to program!).

Next, I briefly describe the technique used to place fine grids in the adaptive model described in Skamarock et al. (1988). The strategy and algorithms were developed at Stanford University and details can be found in Berger and Oliger (1984) and Berger (1982). The grid placement algorithms require a truncation error estimate which is usually provided using the Richardson technique. Using a predetermined error tolerance, points where the error is too large are flagged. Next, the flagged points are divided into clusters. Ideally, the clusters represent spatially distinct reigons of error and usually they are associated with some solution feature. Rectangles are placed around the clusters and these rectangles become the new fine grids. There are three parts to this gridding procedure: flagging the bad points, clustering the points, and placing the grids around the clusters.

Choosing a tolerance for flagging points can be accomplished using theory (see Oliger 1984; Berger 1982), though intuition and experience is used more often. Tolerances are often chosen such that refinements cover reasonable portions of the solution domain. Experience and experimentation may be even more important when using error estimates for all dependent variables in the flagging process. In the simulations of Skamarock et al. (1989) and Caruso (1985), only the velocity error estimates are used. One possible

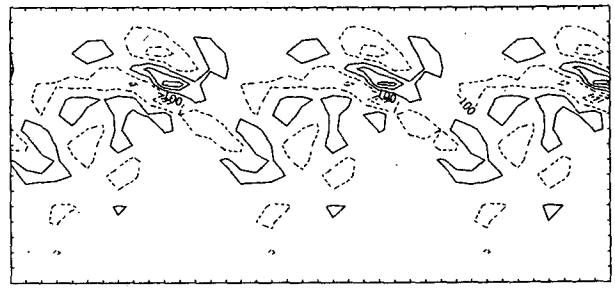

FIG. 13. Truncation error estimate for the temperature equation on the $\sigma = 0.9$ surface using (3.9). Errors normalized and nondimensionalized by dividing by $\Delta t T_0 / t^*$ with $T_0 = 290$ C. Negative contours are dashed and the contour interval is 0.0002 with minimum contours of ± 0.0001.

scheme for using error estimates from all the dependent variables would be to scale and nondimensionalize the error estimates and add them together. The appropriateness and compatibility of the scalings would then be the critical link in the flagging process.

While it is quite easy for a human to look at a set of points and enclose them in a set of rectangles that minimizes the size of the total refined area while, at the same time, producing a small number of rectangles, it is quite difficult to get a computer to perform this task. At present, the points are first clustered using a nearest-neighbor algorithm. If a flagged point is within a critical distance of another flagged point then these points are in the same cluster. All that remains is to choose the critical distance, usually using experience as a guide. More sophisticated procedures may be used if this procedure is inadequate. Inadequacy can be measured by comparing the size of the rectangles to the number of points they contain. The more sophisticated procedures consist of clustering the points using a method more complex than the nearest-neighbor algorithm and then iteratively breaking up the clusters and fitting rectangles until a reasonable set of rectangles is generated. Rectangles are merged as is appropriate.

Fitting rectangles to a specified set of points in some optimal manner is not difficult once the clusters are determined. The essence of the procedure used by Berger (1982) is to compute a least squares fit line through the set of points. This line becomes the principal axis of the rectangle enclosing the points. It is easy to compute where the sides of the rectangle must lie to enclose the points. If rotation is not allowed then it is even easier to compute the enclosing rectangle, but the fit may not be as optimal as that produced by rotating the rectangles.

As an example of grid fitting, Figs. 14 and 15 show the fine grids that were generated by the algorithms using the truncation-error estimate for the u velocity field depicted in Figure 10. The flagged points in Fig. 14 were determined using a tolerance of 0.1. The maximum truncation error in the solution is 0.562. A single fine grid adequately covers the region needing refinement based on this error tolerance. A higher error tolerance, in this case 0.3, is used to generate the fine grids

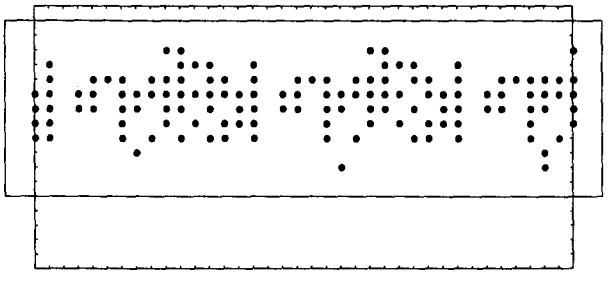

FIG. 14. Flagged points and fine grids generated using the truncation-error estimate in Fig. 10. The error tolerance is 0.1.

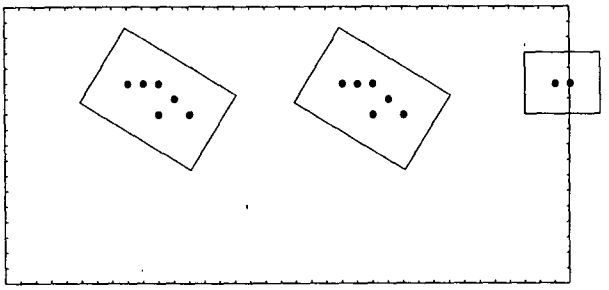

FIG. 15. As in Fig. 14, but with an error tolerance of 0.3.

in Figure 15. Fewer points are flagged and three smaller grids can be used to cover the points. Two of the grids are rotated so as to enclose the flagged points in an efficient manner. The rotated grids also happen to be aligned with the warm fronts associated with the baroclinic disturbances; this will enhance the accuracy of the solution on the fine grids.

In the actual simulation from which the error estimate in Fig. 10 was taken, the error estimate for the other horizontal velocity along with the estimates from all other horizontal planes were used to arrive at the flagged points (see Skamarock et al. 1989). Two overlapping fine grids covered most of the solution domain and flagged points appeared much as in Fig. 14.

Recently, the author has constructed a two-dimensional, nonhydrostatic adaptive model which is being used to study cold pool collapses and the resulting gravity currents. The dry, compressible, Boussinesq equations are used and a complete description of the model can be found in Skamarock (1988b).

Figures 16 and 17 depict a typical cold pool collapse simulated with this model. The domain size, boundary conditions, and resolution of the various grids are given in the figures. The very sharp front at the nose of the gravity current is difficult to resolve, and the Kelvin–Helmholtz (K–H) billows that form in the gravity-current head can be suppressed or may be entirely absent if a coarse discretization is used. Figures 18, 19, and 20 show estimates of the truncation error arising from the spatial discretization of the potential temperature equation, and the horizontal and vertical momentum equations for the largest fine grid. In these simulations, the estimates are computed using finite-difference representations to the leading-order truncation error terms. The front and the two K–H billows are obvious in the truncation-error estimates. Figure 21 shows the points that are flagged based on the three truncation-error estimates and the placement of the finest grids. The finest grids cover the advancing front, the K–H billows, and part of the still-collapsing cold pool.

In this model, as in the previous example involving solutions to the hydrostatic primitive equations, the truncation error is periodically reestimated and the fine grids replaced. Figures 22 and 23 depict the regridding

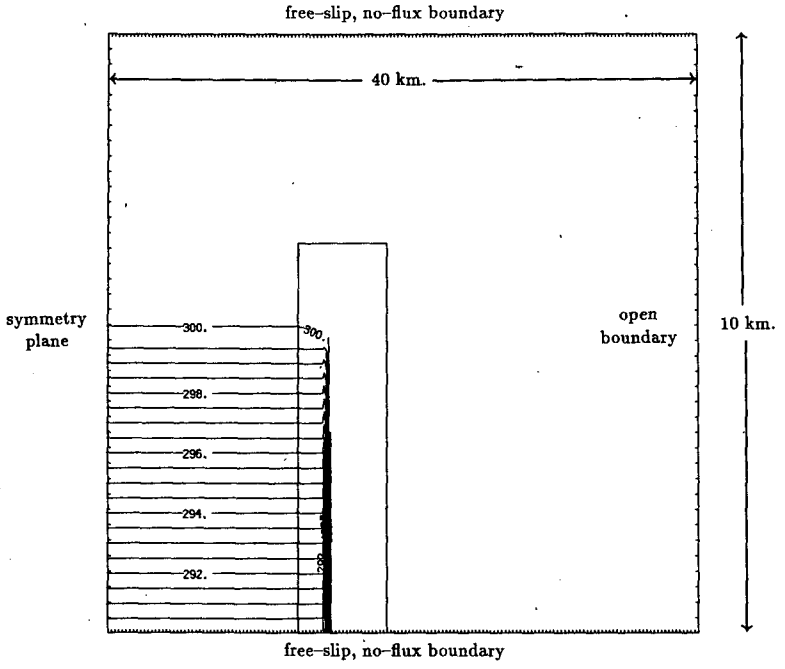

FIG. 16. Potential temperature at time $t = 0$ in the cold pool collapse simulation.

process at a later time. Several K–H billows exist and two are merging. Once again the flagged points (largest errors) are associated with the front and the K–H billows. The solution process is efficient because we minimize the total size of the refined area. This is possible because we use truncation error estimates and multiple fine grids.

Details of the grid fitting procedures are not provided here (see Berger and Oliger 1984) but note that fitting finer grids over regions of high error is the most difficult part of the gridding sequence, and totally satisfactory procedures have not yet been found. Many tasks which

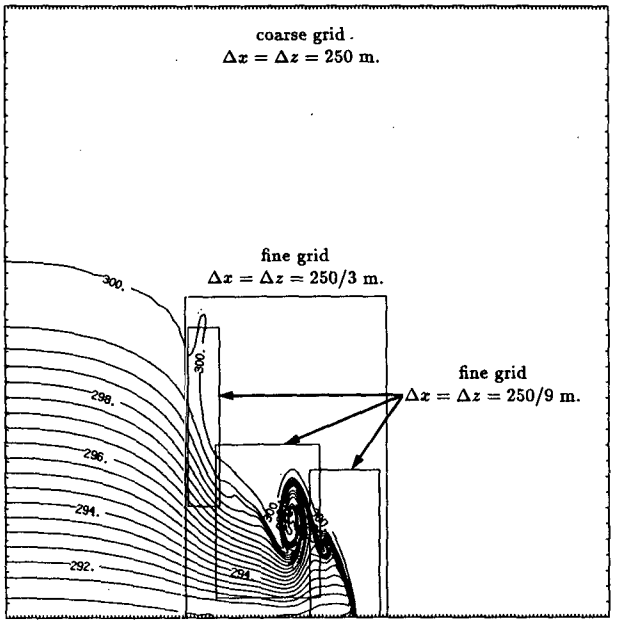

FIG. 17. Potential temperature at $t = 450$ s.

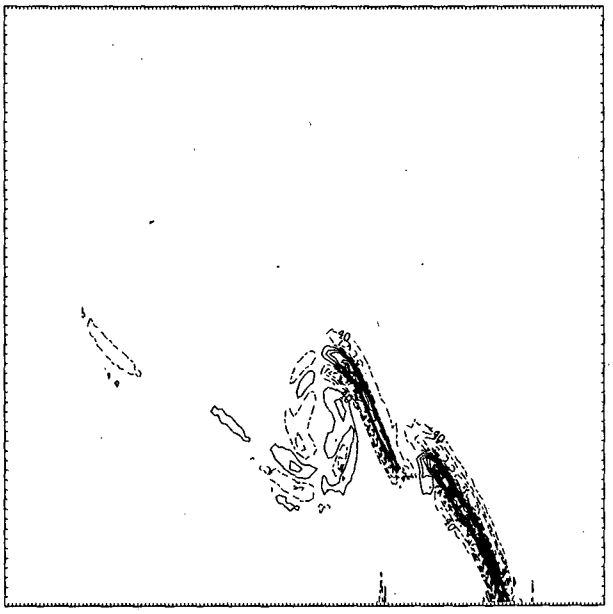

FIG. 18. Truncation error estimate for the spatial discretization in the horizontal momentum equation at $t = 450$ s. The error estimate is for the first inner grid in Figure 17. The units are $m^2 s^{-1}$ with a contour interval of 0.008, and minimum contours of ± 0.004.

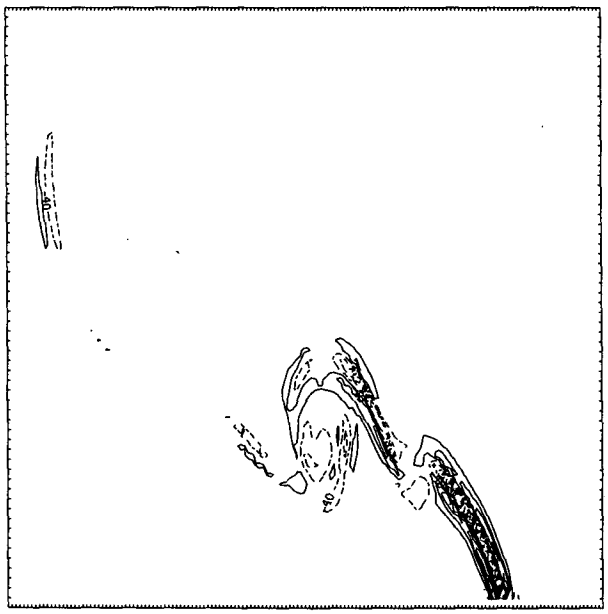

FIG. 19. Truncation error estimate for the vertical momentum equation at t = 450 s. Plotted as in Fig. 18.

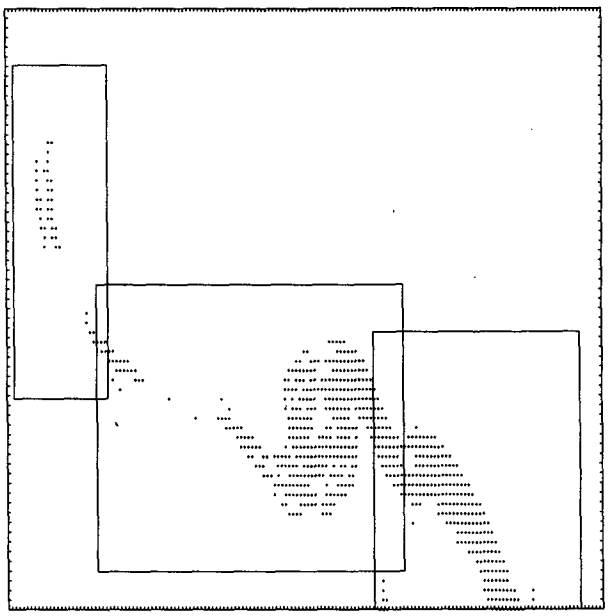

FIG. 21. Flagged points and placement of the finest grids at 450 s based on the truncation error estimates in Figs. 18–20.

are conceptually simple are difficult to program. One possibility which would help circumvent some of the difficulties in the procedures would be to have an interactive model, with the user analyzing the error estimates and then placing the fine grids. Another possibility is to develop an expert system which would control the solution process. It would still encounter the same problems but it may provide sufficient flexibility to include information and algorithms which are not easily included in a standard FORTRAN program. A simple expert system could be developed along the lines of the one developed by Dannenhoffer and

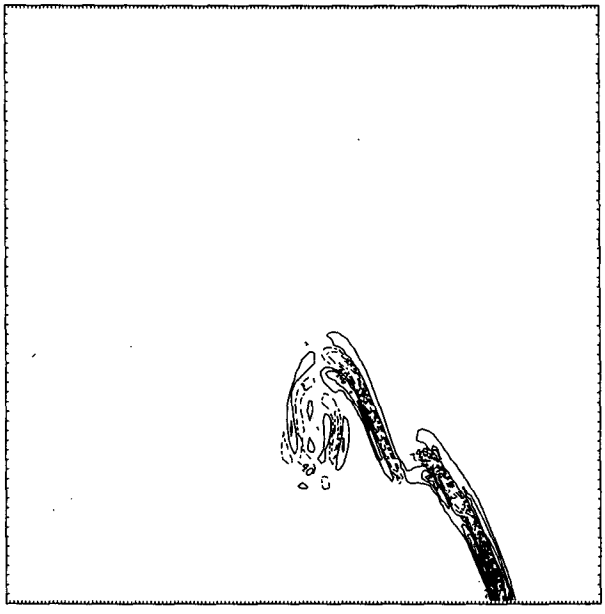

FIG. 20. Truncation error estimate for the potential temperature equation at t = 450 s. The units are s^{-1}, plotted as in Figure 18.

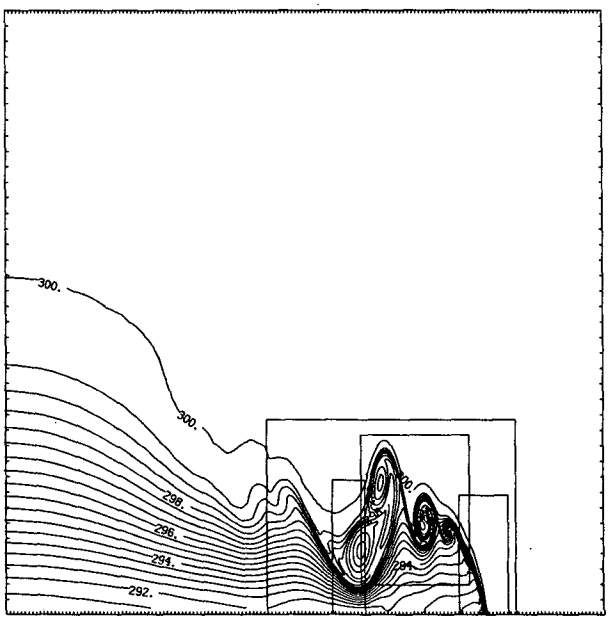

FIG. 22. Potential temperature field at 900 s.

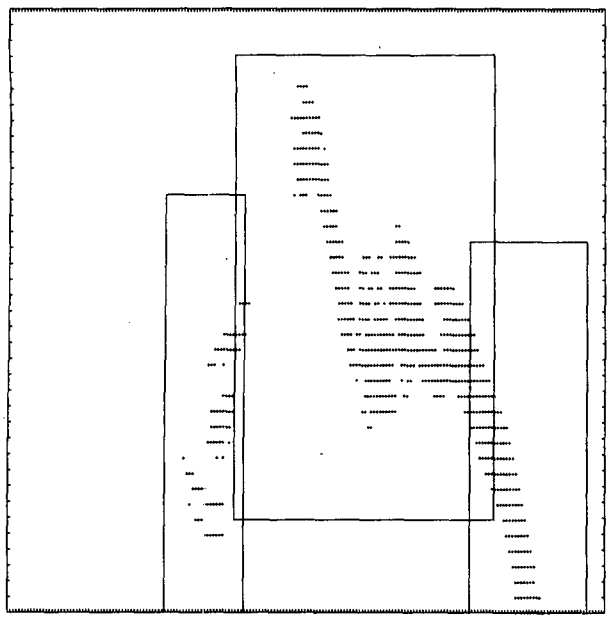

FIG. 23. Flagged points and placement of the finest grids at 900 s. The domain is the first inner grid in Fig. 22.

Baron (1986), although a more complex system would be required to monitor and control the error and solution process continuously.

The adaptive model uses multiple, finer-resolution grids to reduce the truncation error. Other techniques may also be suitable for certain problems. For example, grid points could be clustered in regions of high error using a transformed grid. In an adaptive scheme the grid would be changed periodically in response to the changing truncation error. Present nested models which allow movable grids could use the truncation-error estimates for determining where fine grid(s) should be placed and when the grids should be moved. Most current models use solution features for grid movement and initial grid placement. This does not guarantee solution accuracy. As we have seen, truncation errors may not be large where intuition might expect. Unfortunately, it may not be possible to refine where necessary when only one fine grid of limited size exists. Still, it is best to place the fine grid where the errors are largest, or possibly where the largest amount of error can be enclosed.

As a final point, even when truncation-error estimates are not used for placing fine grids, they can give indications of where large errors exist in the solution. For realistic flows, there are few exact solutions with which to compare model results and it is often prohibitively expensive to compute a grid-independent solution. It is important to observe where truncation errors are large and to consider actual estimates of the errors before considering solutions sufficiently accurate and making inferences about the flow physics. Fortunately, calculating truncation errors using (3.9) is straightforward. As a side note, truncation error estimates for the fine grid domain in two-way interactive nested models can be produced by simply inserting the fine and coarse grid solutions in (3.9) before the coarse grid solution is replaced by the fine grid solution. Equation (3.9) will need to be rederived if the refinement ratio is not 2.

Truncation error estimates can be easily computed. Truncation errors are the source of solution error and more accurate solutions can be obtained by monitoring the errors and using nested or adaptive models to minimize the truncation errors.

Acknowledgments. Part of this work was accomplished while the author was at Stanford University with support from Office of Naval Research Contracts N00014-82-K-0035 and N00014-84-K-0267.

REFERENCES

Babuška, I., J. Chandra and J. E. Flaherty, Eds., 1983: Adaptive computational methods for partial differential equations. *Workshop proceedings,* The Society for Industrial and Applied Mathematics, 251 pp.

Berger, M., 1982: Adaptive mesh refinement for hyperbolic partial differential equations. Doctoral dissertation, Stanford University, Stanford, CA 118 pp.

——, and J. Oliger, 1984: Adaptive mesh refinement for hyperbolic partial differential equations. *J. Comp. Phys.,* **53,** 484–512.

——, and A. Jameson, 1985: Automatic adaptive grid refinement for the Euler equations. *AIAA Journal,* **23,** 561–568.

Bluestein, H., 1986: Fronts and jet streaks, a theoretical perspective. *Mesoscale Meteorology and Forecasting,* P. S. Ray, Ed., Amer. Meteor. Soc., 173–215.

Caruso, S. C., 1985: Adaptive grid techniques for fluid flow problems. Doctoral dissertation, Stanford University, Stanford, CA, 190 pp.

Dannenhoffer, J. F., and J. R. Baron, 1986: Robust grid adaptation for complex transonic flows. *AIAA 24th Aerospace Sciences Meeting Paper AIAA-86-0495.*

Dwyer, H. A., R. J. Kee and B. R. Sanders, 1980: Adaptive grid method for problems in fluid mechanics and heat transfer. *AIAA Journal,* **18,** 1205–1212.

Harrison, E. J., 1973: Three-dimensional numerical simulations of tropical systems utilizing nested finite grids. *J. Atmos. Sci.,* **30,** 1528–1543.

Jones, R. W., 1977: A nested grid for a three-dimensional model a tropical cyclone. *J. Atmos. Sci.,* **34,** 1528–1553.

Kurihara, Y., and M. A. Bender, 1980: Use of a moveable nested-mesh model for tracking a small vortex. *Mon. Wea. Rev.,* **107,** 239–249.

Oliger, J., 1984: Adaptive grid methods for hyperbolic partial differential equations. *Inverse Problems of Acoustic and Elastic Waves,* F. Santosa, Y.-H. Pao, W. W. Symes and C. Holland, Eds., Society for Industrial and Applied Mathematics, 320–331.

Skamarock, W. C., 1988a: Adaptive grid refinement for numerical weather prediction. Doctoral dissertation, Stanford University, Stanford, CA, 126 pp.

——, 1988b: An adaptive and parallel processing model for non-hydrostatic atmospheric flow. Unpublished manuscript.

——, J. Oliger and R. L. Street, 1989: Adaptive grid refinement for numerical weather prediction. *J. Comput. Phys.,* **80**(1), 27–61.